

Quantifying the role of chaperones in protein translocation by computational modelling

Salvatore Assenza, Paolo De Los Rios, and Alessandro Barducci

Laboratoire de Biophysique Statistique, Ecole Polytechnique Fédérale de Lausanne (EPFL), CH-1015 Lausanne, Switzerland

Abstract

The molecular chaperone Hsp70 plays a central role in the import of cytoplasmic proteins into organelles, driving their translocation by binding them from the organellar interior. Starting from the experimentally-determined structure of the *E. coli* Hsp70, we computed, by means of molecular simulations, the effective free-energy profile for substrate translocation upon chaperone binding. We then used the resulting free energy to quantitatively characterize the kinetics of the import process, whose comparison with unassisted translocation highlights the essential role played by Hsp70 in importing cytoplasmic proteins.

Insert Received for publication Date and in final form Date.

Address reprint requests and inquiries to S. Assenza (salvatore.assenza@epfl.ch) or A. Barducci (alessandro.barducci@epfl.ch).

Introduction

Molecular chaperones are protein machines that assist other proteins in various cellular processes. 70-kDa Heat Shock Proteins (Hsp70s) are possibly the most versatile chaperones, supervising a wide variety of cellular tasks (1) that range from disaggregation of stable protein aggregates (2) to driving posttranslational import of cytoplasmic proteins into organelles (3–5). Notably, Hsp70s play a fundamental role in the import of proteins into mitochondria (3). Indeed, the majority of mitochondrial proteins are actually post-translationally imported from the cytosol through outer (TOM) and inner (TIM) membrane pore complexes (3). According to the current view, an ATP-consuming import motor located into the mitochondrial matrix drives the inward translocation of nuclear-encoded proteins. Mitochondrial Hsp70 (mtHsp70) is the central element of this motor: it is recruited by TIM on the matrix side and it binds the incoming protein upon ATP hydrolysis, thus driving its translocation.

The structure of Hsp70 is highly conserved (6) and consists of two large domains connected by a small flexible linker (see fig.1). Specifically, the Nucleotide Binding Domain (NBD) is the ATPase unit of the chaperone, while the Substrate Binding Domain (SBD) directly interacts with specific sites on the incoming protein. These binding sites are frequently found in protein sequences, so that multiple chaperones are likely to bind the same substrate.

The precise mechanism by which Hsp70 exerts its pulling action has been debated in the literature and several models have been proposed (3, 7, 8). The *Brownian ratchet* (3) assumes that, thanks to the chaperone large size, Hsp70 binding prevents the retrotranslocation of the substrate into the pore, thus biasing the random fluctuations toward the matrix. Alternatively, according to the *power stroke* (7) the chaperone actively pulls the incoming protein by using TIM as a fulcrum. Later, according to the *entropic pulling* model (8), it was shown that an active force naturally emerges from a realistic physical description of the Brownian ratchet, thus reconciling the two views (9). Indeed, the excluded volume of the chaperone, besides preventing retrotranslocation, reduces the conformational space available to the incoming protein, thus decreasing its entropy. This reduction depends on the length of the imported fragment of the substrate, therefore resulting in a free-energy gradient which favors the import.

In the present work, we evaluate this thermodynamic force in an effective one-dimensional space where the state of the system is represented by the number n of imported residues. In order to do so, for each value of n we compute the effect

arXiv:1411.6898v1 [q-bio.SC] 25 Nov 2014

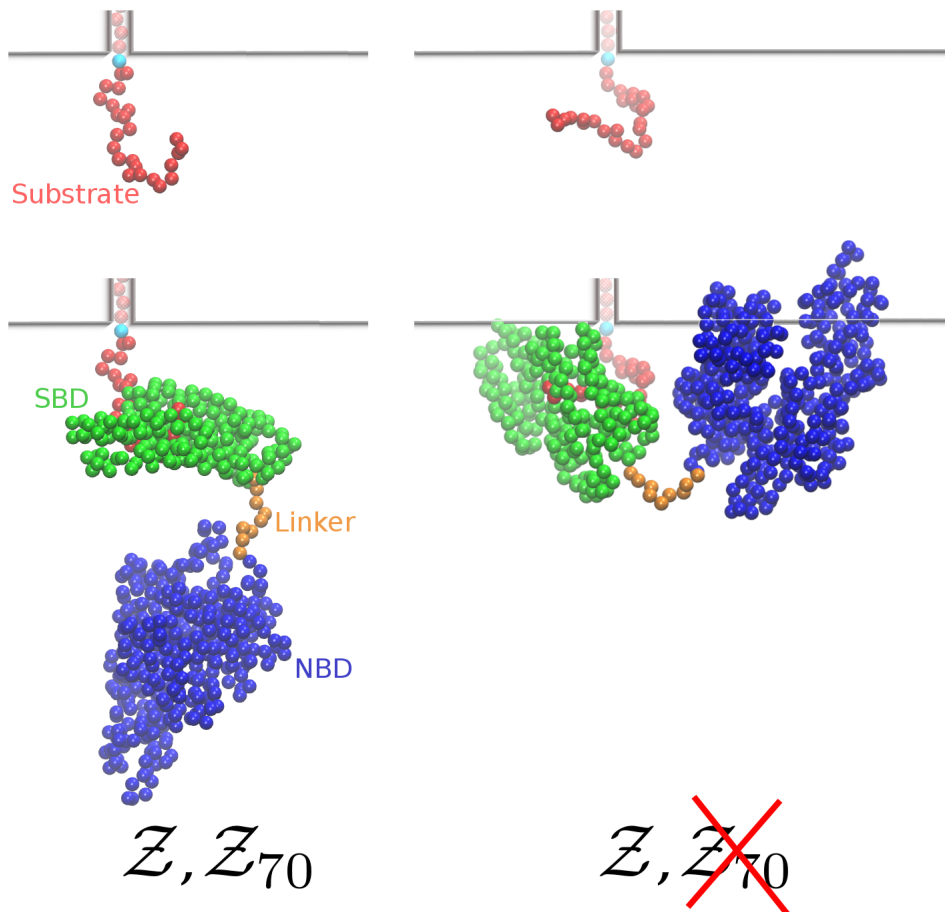


Figure 1: Two representative conformations of the substrate without (top) and with (bottom) bound chaperone. While in the absence of Hsp70s both conformations contribute to $\mathcal{Z}(n)$, upon chaperone binding the one on the right is not taken into account in $\mathcal{Z}_{70}(n)$ due to steric clash with the wall. The n th residue of the substrate, which is constrained on the wall, is colored in cyan. The shaded beads inside the channel are here drawn only for representative purposes.

of chaperone binding on the free energy of the system by means of coarse-grained Molecular Dynamics (MD) simulations. This result is then used to devise a simplified yet quantitative analysis of the import, described as a one-dimensional diffusion process on the computed free-energy landscape.

Methods

Details of MD simulations

We coarse-grained both the substrate and the chaperone by considering one interaction site per residue centered on the C_{α} atom. Residue-residue excluded-volume interactions were modeled with a repulsive Lennard-Jones potential with parameters $\sigma = 3.8 \text{ \AA}$ and $\varepsilon = 3k_B T$. The substrate was modeled by using the local flexible potential introduced in (10). In particular, we made use of the functions denoted as O-X-Y and X-X for the bending and torsional contributions, respectively. The experimental structure of ADP-bound Hsp70 (11) (PDB: 2KHO) was used to model the chaperone. In particular, the NBD (residue 4 to 387) and SBD (residue 397 to 603) were treated as rigid bodies, while the flexibility of the interdomain linker was accounted for by means of the potential described above. In order to reproduce a correct chaperone-substrate arrangement, we took advantage of the substrate-bound X-ray structure of DnaK SBD (PDB: 1DKX (16)).

MD simulations were performed using LAMMPS code (12) at constant temperature ($T = 300 \text{ K}$) by means of a Langevin thermostat with damping parameter equal to 100 fs and using an integration timestep of 10 fs. For each value of n in the range $8 \leq n \leq 26$ we performed a MD simulation of $5 \cdot 10^{10}$ timesteps (examples of the convergence of the ratio $\mathcal{Z}_{70}(n)/\mathcal{Z}(n)$ are reported in the Supplementary Material), and the error on the free-energy profile was estimated by block averaging (13).

Details of the Stochastic Simulations

The import process was simulated by means of a Monte Carlo (MC) algorithm driven by the free-energy landscape F_{import} , as determined from the sum of the chaperones pulling contribution computed by means of the MD simulations and the unfolding free energy F_u . The latter is modeled as a sigmoidal function

$$F_u(n_{\text{in}}) = \frac{F_u^{\text{max}}}{1 + \exp[5 - 10(n_{\text{in}} - 10)/\delta n]},$$

where n_{in} is the total number of imported residues, and F_u^{max} and δn are tunable parameters. For a system at position n_{in} , a trial move was attempted to either $n_{\text{in}} + 1$ or $n_{\text{in}} - 1$ with equal probability and accepted according to the Metropolis criterion based on the free energy F_{import} . To capture the sequence heterogeneity of the proteome, for each choice of F_u^{max} and δn we generated 25 independent binding site distributions, with the sole prescription that the average distance between consecutive binding sites was 35 residues as indicated by experiments (15). For every distribution we performed 10 independent realizations of the import process. Average import times were estimated from MC simulations, that correspond to overdamped Langevin dynamics when only local moves are considered (28, 29). Rescaling the obtained import times by the acceptance rate, as proposed in (14), did not affect the results, because of the large fraction of accepted moves observed in all the simulations (> 95%).

Results

Protein import into organelles has been previously modeled as a one-dimensional stochastic process in the space of the imported residues (17–19). In the present context, this protocol is justified by the timescale separation among substrate conformational dynamics, chaperone binding/unbinding and overall import. Indeed, the typical reconfiguration time of an unfolded protein (~ 100 ns (20)) is extremely fast compared to the experimentally-determined timescale for protein import into mitochondria (order of minutes (21)). Effects arising from substrate conformational dynamics, such as the chaperone-induced entropy reduction, can be thus conveniently represented as effective free-energy profiles influencing the import dynamics. Moreover, the import timescale is also significantly slower than chaperone binding but faster than chaperone unbinding at physiological conditions. Indeed, according to the current understanding of the biochemical cycle of Hsp70 (6, 22), ATP-bound chaperones associate with the substrate with a timescale equal to $\sim 10^{-2}$ s (as estimated from a Hsp70-peptide association rate equal to $4.5 \times 10^5 \text{ M}^{-1}\text{s}^{-1}$ (23) and a chaperone concentration of $70 \mu\text{M}$ in mitochondria (24)), while dissociation takes place from the ADP-bound state, over timescales $\sim 10^3$ s (25). This suggests that, to our purposes, we can assume that a chaperone immediately and irreversibly binds each exposed binding site as soon as it is imported. As a consequence, for the present purposes the number n of substrate residues that have been imported into the mitochondrial matrix is a convenient coordinate to describe the system, whose dynamics can be modeled as a diffusion process on the corresponding free-energy landscape.

Free energy calculation.

The effect of the size of the chaperone is two-fold. On the one hand, bound Hsp70 prevents the retrotranslocation of the substrate beyond its binding point (Brownian ratchet model (3)). On the other hand, the size of the chaperone leads also to a reduced number of sampled conformations (entropic pulling (8)), an effect not accounted for by the Brownian ratchet as it was originally conceived, but nonetheless intimately related to the same physical mechanism. For example, in the absence of Hsp70 the two substrate conformations shown in the top panel of fig.1 are both sterically allowed. However, upon chaperone binding the conformation on the right would result into an overlap between the membrane and Hsp70 (bottom panel in fig.1), and it is therefore never sampled by the substrate when the chaperone is present. The free energy difference due to the loss of entropy is given by $\Delta F_c(n) = -k_B T \log(\mathcal{Z}_{70}(n)/\mathcal{Z}(n))$, where $\mathcal{Z}_{70}(n)$ and $\mathcal{Z}(n)$ are the partition functions of the substrate with and without a bound chaperone, k_B is the Boltzmann constant and T the temperature (when enthalpic contributions are not taken into account, the partition functions reduce to the number of sampled conformations, thus falling back to the original formulation of the entropic-pulling free energy (8)). Here, we computed the free energy difference $\Delta F_c(n)$ by estimating the ratio $\mathcal{Z}_{70}(n)/\mathcal{Z}(n)$ for n in $8 \leq n \leq 26$ with multiple coarse-grained MD simulations. The substrate was modeled as a n -residues flexible chain with the position of the n th residue constrained on the inner mitochondrial membrane, represented here as a flat wall acting only on the substrate residues (see Methods for additional details). As a consequence, the system could sample configurations involving an overlap between the membrane and the chaperone (see bottom-right panel in fig.1). With this strategy, we could estimate the ratio $\mathcal{Z}_{70}(n)/\mathcal{Z}(n)$ as the fraction of time spent by the system in physically-acceptable, *i.e.* non-overlapping, configurations. Particularly, we focused on $n \geq 8$ in order to allow the exposure of a complete binding

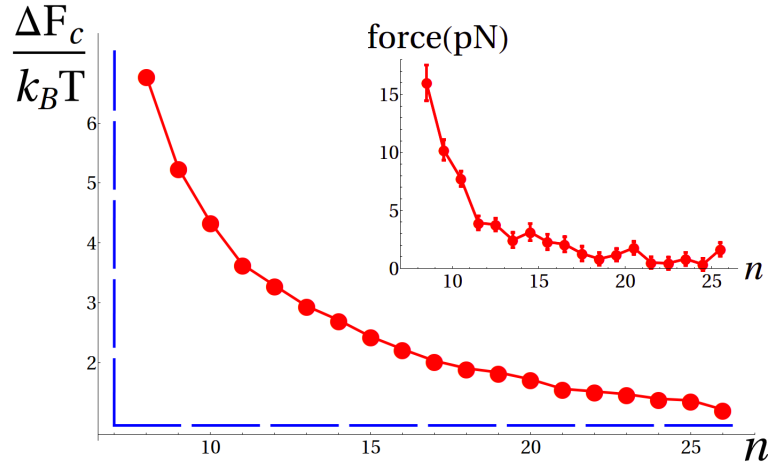


Figure 2: Free-energy profile due to chaperone binding as a function of n (red circles). Error bars are smaller than the size of the symbols. The dashed blue line depicts the free-energy landscape predicted by the original Brownian ratchet, where the only effect of the chaperone is to prevent retrotranslocation beyond the binding site (infinite wall). In the inset we report the thermodynamic force corresponding to the computed free-energy landscape.

site. From the computed values of $Z_{70}(n)/Z(n)$, we could retrieve the free energy $\Delta F_c(n)$ as a function of n , as reported in fig.2. As expected, shorter imported fragments resulted into a larger fraction of rejected conformations, *i.e.* larger values of ΔF_c , thus leading to a free-energy gradient favoring the import of the protein. The slope of the entropic-pulling free-energy profile corresponds to the thermodynamic pulling force exerted by a bound chaperone along n (fig.2 inset). This force is in the piconewton range, starting from around 15 pN and decreasing as n increases. Remarkably, these results agree qualitatively with previous estimates based on strongly simplified representations of the system (8), thus suggesting that comparable thermodynamic forces could be obtained by the same entropic pulling mechanism for macromolecules of similar size.

Stochastic simulations of the import process.

We modeled the import of cytoplasmic proteins as a one-dimensional stochastic process depending on the number n_{in} of imported amino acids. The effective free-energy profile guiding the system evolution results from protein unfolding (26) and active chaperone pulling (21). Assuming a two-states folding behavior, a convenient choice to model the unfolding contribution to the free-energy landscape is a tunable sigmoidal function $F_u(n_{\text{in}})$ (see Methods), depending on two parameters that measure the total unfolding free energy (F_u^{max}) and the cooperativity of the unfolding process (δn), with smaller values of δn corresponding to higher cooperativity (top panel in fig.3). By tuning these parameters, the formula can account for the wide variety of imported proteins (27). The pulling action of the chaperone was modeled taking advantage of the free-energy profile determined from molecular simulations. Particularly, we assumed here that: i) Hsp70s associate with each binding site as soon as it emerges from the pore, since they are targeted at the TIM pore exit by specific interactions (3); ii) we considered only the contribution arising from the Hsp70 closest to the pore, taking into account the relatively fast decrease of the slope of ΔF_c (see fig.2) and the average frequency of binding sites (one every 35 amino acids (15)). Therefore, we added to the unfolding free-energy $F_u(n_{\text{in}})$ the chaperone contribution $\Delta F_c(n_{\text{in}} - n_B)$, with n_B corresponding to the position of the binding site closest to the pore, measured from the matrix terminus of the substrate.

As an example, in the bottom panel of fig.3 we illustrate the evolution of the free-energy landscape during the import process of a protein with $F_u^{\text{max}} = 5k_B T$, $\delta n = 100$ and two binding sites at $n_B = 0$ (*i.e.* at the matrix terminus) and $n_B = 28$. At the beginning of the import process, no chaperone is bound to the substrate and the import free energy is simply given by $F_{\text{import}}(n_{\text{in}}) = F_u(n_{\text{in}})$ (red dashed curve). As soon as the first binding site is imported, a chaperone molecule binds the substrate and its contribution ΔF_c is added to $F_u(n_{\text{in}})$ starting from the binding site $n_B = 0$: $F_{\text{import}}(n_{\text{in}}) = F_u(n_{\text{in}}) + \Delta F_c(n_{\text{in}})$ (purple continuous curve). Finally, after the second binding site ($n_B = 28$) is imported, another chaperone binds and the resulting free energy is $F_{\text{import}}(n_{\text{in}}) = F_u(n_{\text{in}}) + \Delta F_c(n_{\text{in}} - 28)$ (orange dot-dashed curve).

Following this approach, we computed the average import time (see Methods) of 300-residue proteins for different values of δn and a range of F_u^{max} corresponding to the stability of a large fraction of the proteome (30). In absence of Hsp70

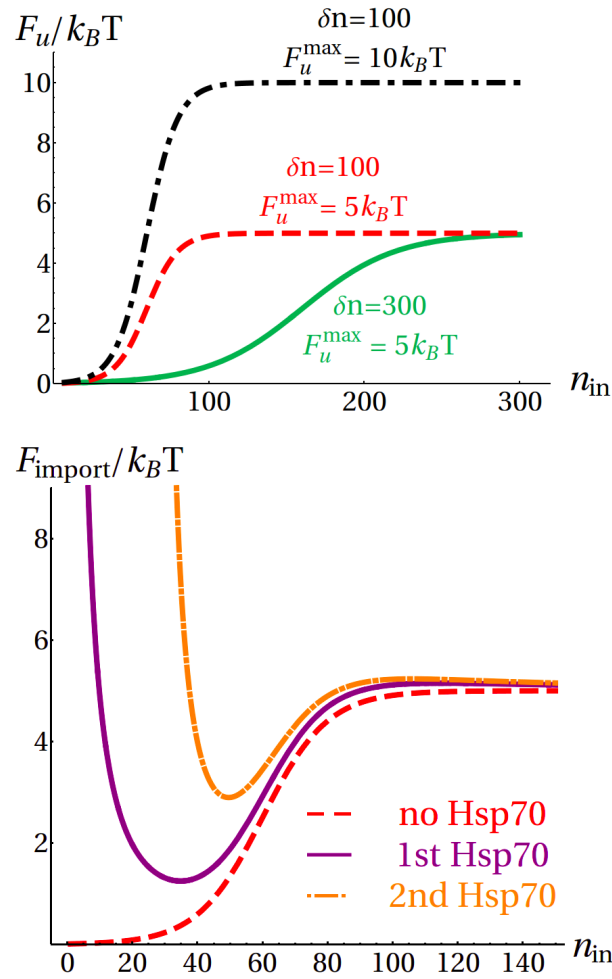


Figure 3: Top: influence of the parameters F_u^{\max} and δn on the unfolding free-energy. Bottom: evolution of the total free-energy F_{import} in a representative import process.

assistance, the system must invariably overcome a free-energy barrier, and the average import time τ_0 increases exponentially with F_u^{\max} , independently of cooperativity (fig.4 top). In all the considered cases, the average import time for the chaperone-assisted process, τ_C , is sensibly smaller than τ_0 (fig.4 center). The chaperone pulling force reduces but does not completely eliminate the unfolding free-energy difference for stable proteins (large F_u^{\max}), as in the case of the representative process shown in the bottom panel of fig.3. In this regime, the import is still an activated process, and the average times increase exponentially with F_u^{\max} . Conversely, the pulling action of Hsp70 dominates over the unfolding contribution for marginally stable proteins (small F_u^{\max}), thus resulting in values of τ_C comparable to what found for the extreme case $F_u^{\max} = 0$. The import kinetics is further modulated by δn , with high cooperativity (small δn) resulting in longer translocation times.

In the bottom panel in fig.4 we illustrate the chaperone-induced kinetic advantage by reporting the ratio τ_0/τ_C . This ratio ranges from a 10-fold gain for marginally stable proteins to 10^3 for extremely stable and noncooperative substrates, with the majority of the proteome ($F_u^{\max} \geq 8 k_B T$ (30)) accelerated at least 100 times. If we take into account that protein import into mitochondria has been measured to happen in the timescale of several minutes (21), our model indicates that the translocation process in the absence of chaperones would probably extend to hours or days. Since such a slow process would clearly be incompatible with the average lifespan of proteins and the duration of the cell cycle, our results provide a molecular basis to support the essential role of chaperones in the *in vivo* import process.

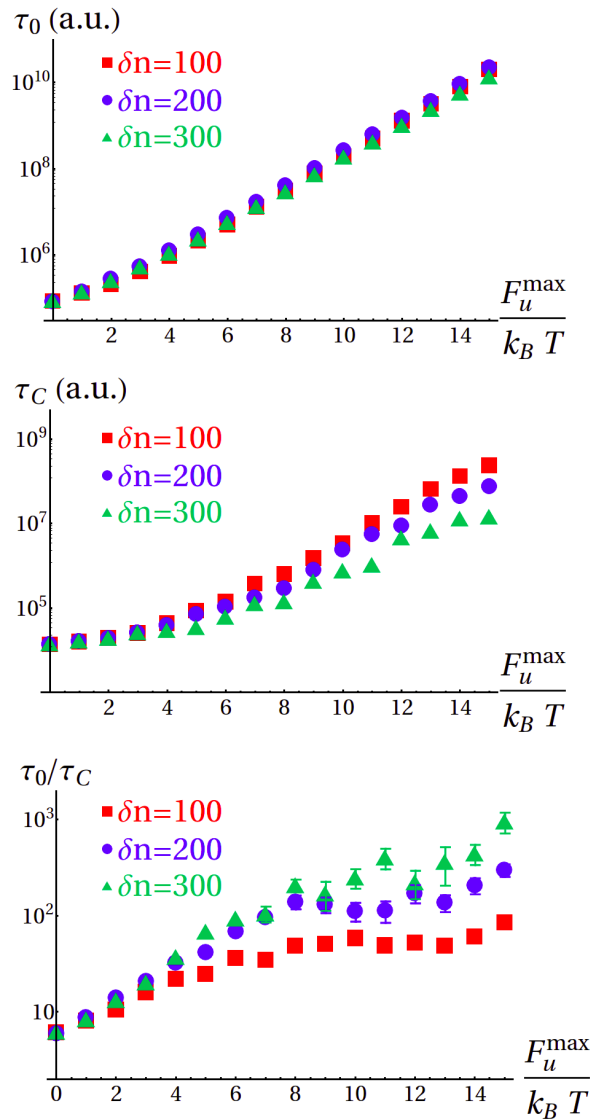


Figure 4: Top: Average import times in the absence of chaperone (τ_0) as a function of F_u^{\max} for different cooperativities (values for $F_u^{\max} \geq 12k_B T$ were extrapolated by fitting the data in the range $4k_B T \leq F_u^{\max} \leq 11k_B T$ with exponential functions). Center: Average import times in the presence of Hsp70 (τ_C) for the same cases as in the top panel. Bottom: Acceleration of the process due to the assistance of Hsp70, expressed as the ratio τ_0/τ_C .

Conclusions

To summarize, in this work we derived a free-energy profile for the import process based on a molecular description of Hsp70 that rationalizes the requirement for chaperone assistance in mitochondrial protein import observed in experiments. The present results can be applied to other cases of Hsp70-driven translocation, namely protein import into ER (4) and chloroplasts (5). Moreover, this approach based on the combination of molecular simulations and kinetic modeling can be easily extended to other Hsp70-mediated cell processes. In particular, this free-energy picture could help to understand some recent results pointing towards a fundamental role of Hsp70 in preventing the stalling of translation at ribosomes (31, 32). Owing to the universality of the interaction responsible for the effects studied here, namely excluded volume, the same principles could apply to similar processes driven by other biomolecules.

AUTHOR CONTRIBUTIONS

S.A., P.D.L.R. and A.B. designed and performed research, analyzed the results and wrote the paper.

ACKNOWLEDGEMENTS

The authors thank the Swiss National Science Foundation for support under the grant 200021-138073 (S.A. and P.D.L.R.) and the Ambizione fellowship program (A.B.).

References

1. Mayer, M. P., and B. Bukau. 2005. Hsp70 chaperones: cellular functions and molecular mechanism. *Cell. Mol. Life Sci.* 62,670.
2. Diamant, S., A. P. Ben-Zvi, B. Bukau, and P. Goloubinoff. 2000. Size-dependent disaggregation of stable protein aggregates by the DnaK chaperone machinery. *J. Biol. Chem.* 14,21107.
3. Neupert W., and M. Brunner. 2002. The Protein Import Motor of Mitochondria. *Nat. Rev. Mol. Cell. Biol.* 3,555.
4. Matlack, K. E., B. Misselwitz, K. Plath, and T. A. Rapoport. 1999. BiP acts as a molecular ratchet during posttranslational transport of prepro-alpha factor across the ER membrane. *Cell* 97,553.
5. Liu, L., R. T. McNeilage, L. X. Shi, and S. M. Theg. 2014. ATP Requirement for Chloroplast Protein Import Is Set by the Km for ATP Hydrolysis of Stromal Hsp70 in *Physcomitrella patens*. *The Plant Cell* 113, 121822.
6. Zuiderweg, E. R. P., E. B. Bertelsen, A. Rousaki, M. P. Mayer, J. E. Gestwicki, and A. Ahmad. 2013. Allostery in the Hsp70 Chaperone Proteins. *Top. Curr. Chem.* 328,99.
7. B. S. Glick. 1995. Can Hsp70 Proteins Act as Force-Generating Motors? *Cell* 80,11.
8. De Los Rios, P., A. Ben-Zvi, O. Slutsky, A. Azem, and P. Goloubinoff. 2006. Hsp70 chaperones accelerate protein translocation and the unfolding of stable protein aggregates by entropic pulling. *Proc. Nat. Acad. Sci.* 103,6166.
9. Goloubinoff, P., and P. De Los Rios. 2007. The mechanism of Hsp70 chaperones: (entropic) pulling the models together. *TRENDS in Biochem. Sci.* 32,372.
10. Ghavami, A., E. Van der Giessen, and P. R. Onck. 2013. Coarse-Grained Potentials for Local Interactions in Unfolded Proteins. *J. Chem. Theory Comput.* 9,432.
11. Bertelsen, E. B., L. Chang, J. E. Gestwicki, and E. R. Zuiderweg. 2009. Solution conformation of wild-type E. coli Hsp70 (DnaK) chaperone complexed with ADP and substrate. *Proc. Nat. Acad. Sci.* 106,8471.
12. S. Plimpton. 1995. Fast Parallel Algorithms for Short-Range Molecular Dynamics. *J. Comput. Phys.* 117,1. <http://lammps.sandia.gov/index.html>
13. Frenkel, D., and B. Smith. 2002. *Understanding Molecular Simulation - 2nd Edition*. Academic Press, San Diego.
14. Sanz, E., and D. Marenduzzo. 2010. Dynamic Monte-Carlo versus Brownian dynamics: a comparison for self-diffusion and crystallization in colloidal fluids. *J. Chem. Phys.* 132,194102.
15. Rüdiger, S., L. Germeroth, J. Schneider-Mergener, and B. Bukau. 1997. Substrate specificity of the DnaK chaperone determined by screening cellulosebound peptide libraries. *EMBO J.* 16,1501.x
16. Zhu, X., X. Zhao, W. F. Burkholder, A. Gragerov, C. M. Ogata, M. E. Gottesman, and W. A. Hendrickson. 1996. Structural analysis of substrate binding by the molecular chaperone DnaK. *Science* 272,1606.
17. Liebermeister, W., T. A. Rapoport, and R. Heinrich. 2001. Ratcheting in Post-translational Protein Translocation: A Mathematical Model. *J. Mol. Biol.* 305,643.
18. Elston, T. 2000. Models of post-translational protein translocation. *Biophys. J.*, 79,2235.
19. Elston, T. 2002. The Brownian ratchet and power stroke models for posttranslational protein translocation into the endoplasmic reticulum. *Biophys. J.*, 82,1239.
20. Soranno, A., B. Buchli, D. Nettels, R. R. Cheng, S. Müller-Späh, S. H. Pfeil, A. Hoffmann, E. A. Lipman, D. E. Makarov, and B. Schuler. 2012. Quantifying internal friction in unfolded and intrinsically disordered proteins with single-molecule spectroscopy. *Proc. Nat. Acad. Sci.* 109,17800.
21. Lim, J. H., F. Martin, B. Guiard, N. Pfanner, and W. Voos. 2001. The mitochondrial Hsp70-dependent import system actively unfolds preproteins and shortens the lag phase of translocation. *The EMBO Journal* 20,941.
22. De Los Rios, P., and A. Barducci. 2014. Hsp70 chaperones are non-equilibrium machines that achieve ultra-affinity by energy consumption. *eLife* 3,e02218.
23. Schmid, D., A. Baici, H. Gehring, and P. Christen. 1994. Kinetics of molecular chaperone action. *Science* 263,971.
24. Liu, Q., P. D'Silva, W. Walter, J. Marszalek, and E. A. Craig. 2003. Regulated Cycling of Mitochondrial Hsp70 at the Protein Import Channel. *Science* 300,139.
25. Mayer, M. P., H. Schröder, S. Rüdiger, K. Paal, T. Laufen, and B. Bukau. 2000. Multistep mechanism of substrate binding determines chaperone activity of Hsp70. *Nat. Struct. Biol.* 7,586.
26. Eilers, M., and G. Schatz. 1986. Binding of a specific ligand inhibits import of a purified precursor protein into mitochondria. *Nature* 322,228.

27. Wilcox, A. J., J. Choy, C. Bustamante, and A. Matouschek. 2005. Effect of protein structure on mitochondrial import. *Proc. Nat. Acad. Sci.* 102,15435.
28. N. G. van Kampen. 1992. *Stochastic Processes in Physics and Chemistry*. North-Holland, Amsterdam.
29. Tiana, G., L. Sutto, and R. A. Broglia. 2007. Use of the Metropolis algorithm to simulate the dynamics of protein chains. *Physica A* 380,241.
30. Ghosh, K., and K. Dill. 2010. Cellular Proteomes Have Broad Distributions of Protein Stability. *Biophys. J.* 99,3996.
31. Liu, B., Y. Han, and S. Qian. 2013. Cotranslational Response to Proteotoxic Stress by Elongation Pausing of Ribosomes. *Mol. Cell* 49,453.
32. Shalgi R., A. J. Hurt, I. Krykbaeva, M. Taipale, S. Lindquist, and C. B. Burge. 2013. Widespread Regulation of Translation by Elongation Pausing in Heat Shock. *Mol. Cell* 49,439.